Journal of Medicinal Chemistry

ARTICLE

pubs.acs.org/jmc

Highly Improved Metabolic Stability and Pharmacokinetics of Indium-111-DOTA-Gastrin Conjugates for Targeting of the Gastrin Receptor

Petra Kolenc-Peitl,[†] Rosalba Mansi,[‡,#] MariaLuisa Tamma,[‡] Tanja Gmeiner-Stopar,[†] Marija Sollner-Dolenc,[∥] Beatrice Waser,[⊥] Richard P. Baum,[§] Jean Claude Reubi,[⊥] and Helmut R. Maecke*[,‡,#]

[†]Department of Nuclear Medicine, University Medical Centre Ljubljana, Zaloška Cesta 7, SI-1000 Ljubljana, Slovenia

[‡]Division of Radiological Chemistry, University Hospital Basel, Petersgraben 4, CH-4031 Basel, Switzerland

[§]Department of Nuclear Medicine/PET Center, Zentralklinik Bad Berka, Bad Berka, Germany

[∥]Faculty of Pharmacy, University of Ljubljana, Aškerčeva Cesta 7, SI-1000 Ljubljana, Slovenia

[⊥]Division of Cell Biology and Experimental Cancer Research, Institute of Pathology, University of Berne, Murtenstrasse 31, CH-3010 Berne, Switzerland

[#]Department of Nuclear Medicine, University of Freiburg, Hugstetterstrasse 55, 79106 Freiburg, Germany

Supporting Information

ABSTRACT: The development of metabolically stable radiolabeled gastrin analogues with suitable pharmacokinetics is a topic of recent research activity. These imaging vectors are of interest because the gastrin/CCK2 receptor is highly overexpressed in different tumors such as medullary thyroid cancer, neuroendocrine tumors, and SCLC. The drawback of current targeting agents is either their metabolic instability or their high kidney uptake. We present the synthesis and in vitro and in vivo evaluation of 11 ^{111}In-labeled DOTA-conjugated peptides that differ by their spacer between the peptide and the chelate. We introduced uncharged but hydrophilic spacers such as oligoethyleneglycol, serine, and glutamine. The affinity of all radiopeptides was high with IC_{50} values between 0.5 and 4.8 nM. The improvement of human serum stability is 500-fold within this series of compounds. In addition the kidney uptake could be lowered distinctly and the tumor-to-kidney ratio improved almost 60-fold if compared with radiotracers having charged spacers such as glutamic acid.

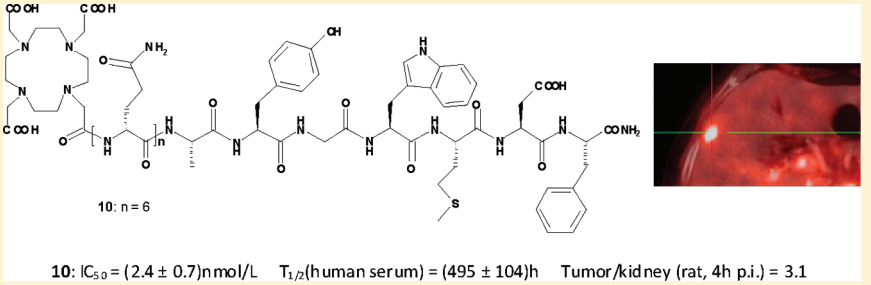

INTRODUCTION

The gastrin receptor is shown to be important and of high relevance to human physiology and pathophysiology. A comprehensive overview was given recently by Dufresne et al.[1] This receptor is highly expressed in several tumor types, including neuroendocrine tumors (in particular medullary thyroid cancer (MTC) and small cell lung cancer, SCLC).[2] These tumors can be visualized by imaging techniques such as positron emission tomography (PET) and single photon emission computed tomography (SPECT) by use of corresponding radiolabeled gastrin analogues or treated with peptide receptor radionuclide therapy (PRRT) if labeled with a particle emitter. In recent years clinical studies have emphasized the role of gastrin receptor scintigraphy for tumor detection in patients with metastasized MTC or neuroendocrine tumors (NETs) when somatostatin receptor scintigraphy had failed.[3] Although there are minigastrin (MG) (LEEEEEAYGWMDF-NH_2) analogues suitable for diagnostic purposes, candidates for PRRT still need to be found. The main limiting factor is the low tumor uptake[4] or the too high kidney retention that can cause nephrotoxicity.[5]

MG analogues with reduced number of glutamic acid residues (reduced negative charge) show improved tumor-to-kidney ratios. The drawback of truncated MG analogues is the low enzymatic stability in human serum[6] which makes them poor candidates for clinical use.[4,7] These findings indicate the important role of the spacer length and chemical composition on kidney uptake and on metabolic stability. Successful approaches to improve the metabolic stability of linear peptides include introduction of D-amino acids, N-methylation, and cyclization.[8,9] In addition polyvalency may be a means to reduce the action of enzymes on peptides and therefore increase metabolic stability.[10] Spacers with different polarity were introduced into radiopeptides, and their effect on pharmacokinetic was studied.[11]

Received: October 5, 2010

   dx.doi.org/10.1021/jm101279a | J. Med. Chem. XXXX, XXX, 000–000

Table 1. Analytical Data of the Studied MG Analogues

compd	amino acid sequence	purity (%)	HRMS	HPLC[a]
1	DOTA-PEG_4-Ala-Tyr-Gly-Trp-Met-Asp-Phe-NH_2	97.6	1521.6942 [M + H^+]	22.58
2	DOTA-PEG_6-Ala-Tyr-Gly-Trp-Met-Asp-Phe-NH_2	98.4	1609.7461 [M + H^+]	22.92
3	DOTA-(D-Ser)$_2$-Ala-Tyr-Gly-Trp-Met-Asp-Phe-NH_2	97.9	1448.6154 [M + H^+]	22.95
4	DOTA-(D-Ser)$_3$-Ala-Tyr-Gly-Trp-Met-Asp-Phe-NH_2	98.4	1535.6479 [M + H^+]	22.70
5	DOTA-(D-Gln)$_2$-Ala-Tyr-Gly-Trp-Met-Asp-Phe-NH_2	97.9	1530.6689 [M + H^+]	22.50
6	DOTA-(D-Gln)$_3$-Ala-Tyr-Gly-Trp-Met-Asp-Phe-NH_2	98.5	1658.7275 [M + H^+]	22.30
7	DOTA-PEG_{12}-Ala-Tyr-Gly-Trp-Met-Asp-Phe-NH_2	98.4	1873.9035 [M + H^+]	23.05
8	DOTA-(D-Gln)$_3$-Ala-Tyr-Gly-Trp-Nle-Asp-Phe-NH_2	98.9	1640.7709 [M + H^+]	23.57
9	DOTA-(D-Gln)$_4$-Ala-Tyr-Gly-Trp-Met-Asp-Phe-NH_2	98.4	1786.7858 [M + H^+]	22.17
10	DOTA-(D-Gln)$_6$-Ala-Tyr-Gly-Trp-Met-Asp-Phe-NH_2	99.5	2042.9032 [M + H^+]	22.20
11	DOTA-(L-Glu)$_6$-Ala-Tyr-Gly-Trp-Met-Asp-Phe-NH_2	99.2	2048.8072 [M + H^+] ESI-MS	27.50
^{nat}In-**2**	^{nat}In-DOTA-PEG_6-Ala-Tyr-Gly-Trp-Met-Asp-Phe-NH_2	99.7	1723.3 [M + H^+]	28.30
^{nat}In-**10**	^{nat}In-DOTA-(D-Gln)$_6$-Ala-Tyr-Gly-Trp-Met-Asp-Phe-NH_2	99.6	1078.2 [M + $2H^+$]/2	23.40

[a] Used HPLC gradient system as described in Experimental Section.

Table 2. Gastrin Receptor Binding Affinities, Serum Stabilities, and Internalization Rates of the ^{111}In-Labeled Analogues

compd	IC_{50} (nmol/L)	$T_{1/2}$ (h)[a]	% internalization rate[b]	% cellular retention[c]	EC_{50} (nmol/L)
1	3.4 ± 1.0 (2)	1.0 ± 0.2 (n = 2)	6.6 ± 0.5 (n = 2)		
2	2.5 ± 0.9 (2)	1.8 ± 0.6 (n = 5)	7.7 ± 0.7 (n = 2)		0.33
3	0.9 ± 0.3 (3)	2.7 ± 1.2 (n = 2)	11.3 ± 0.3 (n = 2)		
4	0.6 ± 0.1 (3)	2.9 ± 0.5 (n = 2)	12.5 ± 2.4 (n = 2)		
5	0.8 ± 0.1 (3)	9.4 ± 0.5 (2)	9.8 ± 0.2 (2)		
6	3.6 ± 0.6 (3)	25.3 ± 3.8 (3)	11.9 ± 1.9 (4)	70.7 ± 11.9 (n = 2)	0.27
7	4.8 ± 0.4 (3)	3.1 ± 1.0 (2)	4.6 ± 0.6 (2)		
8	1.6 ± 0.8 (3)	9.7 ± 1.6 (2)	10.2 ± 3.2 (2)		
9	2.4 ± 0.7 (2)	65 ± 54 (3)	13.0 ± 3.6 (3)		
10	2.4 ± 1.1(2)	495 ± 104 (3)	12.8 ± 3.7 (4)	76.8 ± 5.9 (n = 2)	0.41
11	0.7 ± 0.2 (3)	75.0 ± 23 (2)	14.4 ± 0.8 (2)		
^{nat}In-**2**	2.5 ± 1.1 (3)				
^{nat}In-**10**	2.6 ± 0.3 (3)				

[a] Enzymatic stabilities in serum are expressed as half-life in hours. [b] Internalization rates are expressed as percentage of injected activity per million cells (mean ± SD). [c] Cellular retention is expressed as percentage of activity retained in the cells with regard to specific internalized fraction; number of independent studies is listed in parentheses.

Our hypothesis was that one may improve metabolic stability and pharmacokinetics by introducing hydrophilic but uncharged spacers of different lengths. Macrocyclic chelators like 1,4,7,10-tetraazacyclododecane-1,4,7,10-tetraacetic acid (DOTA) provide high complex stability.[6] We present herein DOTA-coupled MG analogues for the labeling with +3 charged radiometals. We examine how the introduction of nonionic spacers influence the metabolic stability and therefore the pharmacokinetic profile of the new analogues. The reported ^{111}In-DOTA-coupled peptides show human serum stability half-lives that differ almost 500-fold. The kidney uptake was reduced distinctly if compared to corresponding peptides with highly charged spacers, and the tumor-to-kidney ratios are increased.

RESULTS

Synthesis and Radiolabeling. The peptides were synthesized on solid phase using standard Fmoc chemistry. All conjugates showed purities over 95% as confirmed by reversed-phase high-performance liquid chromatography (RP-HPLC). All of the peptides, including the two metalated candidates, were characterized by electrospray ionization mass spectrometry (ESI-MS), high resolution mass spectrometry (HRMS), and RP-HPLC (Table 1). Radiochemical purity of >95% at specific activities of >37 GBq μmol^{-1} were achieved for all the conjugates.

Binding Affinity Studies on Cholecystokinin-1- (CCK-1) and Gastrin-Receptor Expressing Tissues. Receptor binding affinities to CCK-1 and gastrin receptor positive tumor cells are compiled in Table 2 and expressed as IC_{50} using ^{125}I-D-Tyr-Gly-Asp-Tyr-(SO_3H)-Nle-Gly-Trp-Nle-Asp-Phe-NH_2 (^{125}I-CCK) as reference ligand. All compounds show IC_{50} between 0.5 and 4.8 nmol/L to the gastrin receptor and >700 nmol/L to the CCK-1 receptor. Replacement of methionine with norleucine (DOTA-(D-Gln)$_3$-Ala-Tyr-Gly-Trp-Met-Asp-Phe-NH_2 (DOTA-(D-Gln)$_3$-gastrin-7, **6**) vs DOTA-(D-Gln)$_3$-[Nle^5]-gastrin-7 (**8**) results in 2-fold improvement of the IC_{50}. Metalation of the chelator does not affect binding affinity in the two selected cases; the IC_{50} values practically do not change in the case of ^{nat}In-DOTA-poly(oxyethylene)$_6$-gastrin-7 (^{nat}In-DOTA-PEG_6-gastrin-7, ^{nat}In-**2**) and ^{nat}In-DOTA-(D-Gln)$_6$-gastrin-7 (^{nat}In-**10**) vs nonmetalated peptides. We assume this is the case also for the remaining peptides.

dx.doi.org/10.1021/jm101279a |J. Med. Chem. XXXX, XXX, 000–000

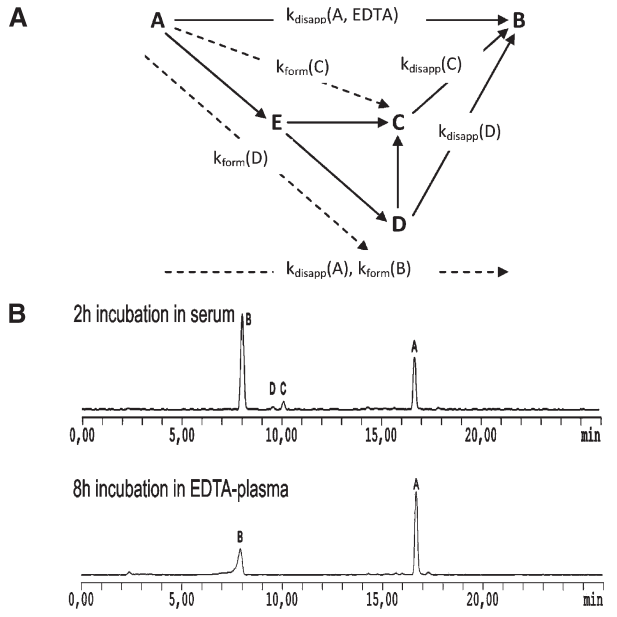

Figure 1. (A) Proposed degradation scheme of ^{111}In-**2**. Metabolites are ^{111}In-DOTA-PEG$_6$-Ala-OH (metabolite B), ^{111}In-DOTA-PEG$_6$-Ala-Tyr-OH (metabolite C), ^{111}In-DOTA-PEG$_6$-Ala-Tyr-Gly-OH (metabolite D), and ^{111}In-DOTA-PEG$_6$-Ala-Tyr-Gly-Trp-Met-NH$_2$ (metabolite E). k_{form} and k_{disapp} are formation and disappearance rate constants. (B) HPLC elution profile of ^{111}In-**2** (A) after 2 h of incubation in human serum (t_r = 16.7 min, t_r(metabolite B) = 8.0 min, t_r(metabolite C) = 10.1 min, t_r(metabolite D) = 9.6 min) and after 8 h of incubation in EDTA-plasma (t_r(substance A) = 16.7 min, t_r-(metabolite B) = 7.9 min.

Enzymatic Stability in Human Serum and Identification of Metabolites. Calculated half-lives of the radiolabeled MG analogues in human blood serum are listed in Table 2. They vary between 1.0 ± 0.2 h (^{111}In-DOTA-PEG$_4$-gastrin-7, ^{111}In-**1**) and 495 ± 104 h (^{111}In-**10**). To understand the large difference, we studied the metabolic degradation of one of the most labile representatives, ^{111}In-**2** (Table 2S), and compared it with the most stable compounds ^{111}In-**10** and ^{111}In-**6**. We identified three metabolites, ^{111}In-DOTA-PEG$_6$-Ala-OH (metabolite B), ^{111}In-DOTA-PEG$_6$-Ala-Tyr-OH (metabolite C), and ^{111}In-DOTA-PEG$_6$-Ala-Tyr-Gly-OH (metabolite D). The degradation scheme of ^{111}In-**2** is shown in Figure 1A.

The disappearance rate constant of the parent peptide k_{disapp}-(A) is in the range of the formation rate for B (0.445 ± 0.067 h^{-1}, n = 2), C (0.417 ± 0.088) h^{-1}, n = 2), and D (0.645 ± 0.215 h^{-1}, n = 2 (k_{disapp}(A) ≈ k_{form}(B) ≈ k_{form}(C) ≈ k_{form}(D), Table 1S). D is very unstable (k_{disapp}(D) = 12.5 ± 1.31 h^{-1}). On the other hand the disappearance rate of B is negligible (k_{disapp}(B) = 0.003 ± 0.001 h^{-1}, n = 2) and k_{disapp}(C) amounts to 0.028 ± 0.000 h^{-1} (n = 2), Table 1S. When metabolite B is incubated in human blood serum, it shows practically no degradation. Metabolite C slowly (0.016 h^{-1}) degrades into B and metabolite D quickly (6.8 h^{-1}) degrades into B. When possible metabolites ^{111}In-DOTA-PEG$_6$-Ala-Tyr-Gly-Trp-OH and ^{111}In-DOTA-PEG$_6$-Ala-Tyr-Gly-Trp-Met-Asp-OH are incubated in human blood serum, they showed higher enzymatic stability compared to metabolite D and are not identified on HPLC as degradation products of the parent peptide. On the other hand ^{111}In-DOTA-PEG$_6$-Ala-Tyr-Gly-Trp-Met-OH (metabolite E) incubated for 10 min in serum did not exhibit any intact peptide but metabolites B, C, and D. When ^{111}In-**2** is incubated in EDTA-plasma, the half-life increased from 1.7 to 7.9 h (Figure 1B). Further on, when C, D, and E are incubated in EDTA-plasma, there was practically no degradation observed. A similar degradation pathway was observed for ^{111}In-**6**, while ^{111}In-**10** shows higher stability and less metabolites.

Circular Dichroism (CD) Spectroscopy. The CD spectrum of ^{nat}In-**2** in water shows two principal bands, one positive around 225−230 nm and one negative at 195 nm (Figure 2). This spectrum is characteristic of a random coil conformation with a small red shift of the positive band that can be ascribed to the aromatic contribution of the Tyr and Trp residues.[12] The addition of 2,2,2-trifluoroethanol (TFE) induced changes in the conformational preferences of the peptide, enhancing its propensity to assume an α-helical conformation. TFE is known to preferentially stabilize proteins and peptides in a helical conformation, favoring the formation of a more ordered conformation by lowering the dielectric constant of the medium. With the addition of 80% TFE the peptide reaches the maximum of ellipticity; its CD spectrum showed two negative bands at 208 and 222 nm and a positive band at 192 nm, typical of α-helical structures. The CD spectrum of ^{nat}In-**10** shows two positive bands at 195 and 225 nm and a weak negative band at 215 nm (Figure 2). We assigned this to a type II reverse turn based on model spectra reported by Reed et al.[13] The spectra registered in several solvents showed intensity differences related to the polarity of the solvent.

In Vitro Internalization and Cellular Retention Studies. The internalized fractions, expressed as percent of the added activity per 1 million cells over 4 h, are listed in Table 2. The 4 h values of all compounds significantly decreased to less than 0.5% after addition of excess unlabeled peptide (p < 0.01). The surface-bound radioligand did not exceed 1.5% of the added radioactivity after 4 h of incubation.

Cellular retention data of the selected peptides ^{111}In-**6** and ^{111}In-**10** are listed in Table 2. The externalization kinetics was assessed after 2 h of internalization of the radioligand. Up to 60 min, the two peptides showed insignificant differences in the externalization rate. At 4 h, 76.8 ± 5.9% and 70.7 ± 11.9% of internalized activity were retained within the cells for ^{111}In-**10** and ^{111}In-**6**, respectively.

Calcium Mobilization Assay. 10, **6**, and **2** were evaluated for their effect on signaling by using a Ca^{2+} flux assay on AR4-2J cells. In the same assay the agonists gastrin (I) rat and pentagastrin and the antagonist proglumide were tested as positive and negative controls. A sigmoidal dose response curve (see Supporting Information Figure 1S) was obtained indicating that the Ca^{2+} response was dependent on peptide concentration. EC_{50} values of 0.41, 0.27, 0.33, 0.16, and 0.17 nmol/L for **10**, **6**, **2**, gastrin (I) rat, and pentagastrin were calculated using a four-parameter fitting equation. As expected, no response was registered for the gastrin receptor antagonist proglumide. **10**, **6**, gastrin (I) rat, and pentagastrin induced comparable maximal levels of Ca^{2+} flux. **2** causes a smaller maximal level of Ca^{2+} flux which indicates that this MG analogue shows properties of partial agonism in accordance with the lower internalization rate of dPEG$_n$ MG analogues of our series.

Biodistribution Studies in AR4-2J Tumor Bearing Lewis Rats. Biodistribution studies using ^{111}In-**6** and ^{111}In-**10** were performed with Lewis male rats bearing AR4-2J rat pancreatic tumor cells and followed for 1, 4, 24, and 48 h. For comparison, biodistribution at 4 and 24 h pi of highly charged

dx.doi.org/10.1021/jm101279a |J. Med. Chem. XXXX, XXX, 000–000

Table 3. Biodistribution Data of ^{111}In-6, ^{111}In-10, and ^{111}In-11[a]

		^{111}In-**6** (%IA/g tissue ± SD)		^{111}In-**10** (%IA/g tissue ± SD)		^{111}In-**11** (%IA/g tissue ± SD)	
organ	time	nonblocked	blocked*	nonblocked	blocked*	nonblocked	blocked*
tumor	1	1.75 ± 0.42		2.40 ± 0.39			
	4	1.24 ± 0.24	0.11 ± 0.003†	1.03 ± 0.43	0.16 ± 0.03‡	2.25 ± 0.23	0.58 ± 0.35
	24	0.47 ± 0.11		0.37 ± 0.08		0.90 ± 0.41	
	48	0.29 ± 0.01		0.43 ± 0.24			
blood	1	0.16 ± 0.05		0.23 ± 0.05			
	4	0.002 ± 0.0001	0.002 ± 0.001	0.003 ± 0.002	0.02 ± 0.006	0.01 ± 0.001	0.01 ± 0.004
	24	0.001 ± 0.0001		0.001 ± 0.0001		0.006 ± 0.003	
	48	0.001 ± 0.0001		0.001 ± 0.0001			
kidney	1	0.80 ± 0.18		0.96 ± 0.13			
	4	0.36 ± 0.03§	0.42 ± 0.07	0.33 ± 0.05‖	0.52 ± 0.053	25.51 ± 2.57	24.86 ± 5.78
	24	0.30 ± 0.02		0.32 ± 0.02		19.35 ± 5.58	
	48	0.32 ± 0.02		0.35 ± 0.07			
liver	1	0.08 ± 0.03		0.13 ± 0.02			
	4	0.03 ± 0.003	0.03 ± 0.01	0.02 ± 0.003	0.06 ± 0.01	0.05 ± 0.01	0.04 ± 0.01
	24	0.02 ± 0.001		0.02 ± 0.004		0.01 ± 0.003	
	48	0.02 ± 0.002		0.02 ± 0.007			
stomach	1	0.21 ± 0.05		0.31 ± 0.03			
	4	0.09 ± 0.05	0.02 ± 0.001	0.13 ± 0.03	0.02 ± 0.002	0.50 ± 0.03	0.12 ± 0.07
	24	0.04 ± 0.02		0.08 ± 0.02		0.03 ± 0.009	
	48	0.04 ± 0.02		0.04 ± 0.02			

	ratio		
parameter	^{111}In-**6** (1 h, 4 h, 24 h, 48 h pi)	^{111}In-**10** (1 h, 4 h, 24 h, 48 h pi)	^{111}In-**11** (4 h, 24 h pi)
tumor/kidney	2.2, 3.4, 1.5, 0.9	2.5, 3.1, 1.2, 1.2	0.09, 0.05
tumor/stomach	8.1, 13.7, 12.7, 7.5	7.81, 7.69, 4.41, 9.54	4.5, 3.4
tumor/liver	21.1, 47.6, 30.1, 17.3	18.9, 49.2, 20.8, 19.1	49.4, 21.9

[a] Uptake as percentage of injected activity per gram of tissue (mean value ± SD). (*) Blocked with 2000 times excess of unlabelled (cold) analogue. (†) $p < 0.01$ vs unblocked ^{111}In-**6**. (‡) $p < 0.01$ vs unblocked ^{111}In-**10**. (§) $p < 0.01$ vs kidney uptake of ^{111}In-**11**. (‖) $p < 0.01$ vs kidney uptake of ^{111}In-**11**.

^{111}In- DOTA-(L-Glu)$_6$-gastrin-7 (^{111}In-**11**) was performed. The data and tumor-to-tissue ratios are summarized in Table 3 and Table 2S. Rapid clearance from all gastrin receptor negative tissues and blood was observed. The kidneys present the main excretory pathway of these radiopeptides. ^{111}In-**10** shows a faster tumor washout compared to ^{111}In-**6**. At 4 h pi ^{111}In-**11** shows 2-fold higher tumor uptake that remains higher at 24 h compared to ^{111}In-**6** and ^{111}In-**10**. The main difference was in the almost 70-fold higher kidney uptake of ^{111}In-**11** at 4 h, resulting in a tumor-to-kidney ratio of 0.09 compared to 3.4 and 3.1 for ^{111}In-**6** and ^{111}In-**10**, respectively. Uptake in the gastrin receptor rich tissues and in the tumor was found to be significantly reduced in the animals preinjected with an excess of cold peptides, indicating a specific receptor mediated uptake.

First Human Study with ^{68}Ga-10. A 59-year-old female patient had been operated in 1992 because of an MTC, possibly hereditary in origin, as the mutation K808 E (AAA > GAA) had been proven in heterozygous constellation later on. She had undergone thyroidectomy and external beam radiation therapy and thereafter repeated resection of cervical lymph node metastases. The patient presented now elevated calcitonin (1830 pg/mL) and CEA (75.4 ng/mL) serum levels. After written informed consent was obtained, a whole-body PET/computed tomography (CT) scan was performed. A gastrin receptor positive liver metastasis (Figure 3 and Figure 2S of the Supporting Information) was detected in liver segment 5 (standardized uptake value, $SUV_{max} = 1.7$) which was in accordance with a previous ^{68}Ga-DOTA-[Tyr^3]octreotide PET/CT. SUVs determined in normal tissue (e.g., liver (1.0), lung (0.5), and gluteus muscle (0.5)) were low except for the stomach mucosa (3.1).

DISCUSSION

There is currently no effective therapy available for patients with distant metastases of MTC. Different attempts have been made to develop gastrin analogues suitable for imaging and PRRT of MTC and other gastrin receptor expressing tumors. The main problem is the high kidney retention of these radiolabeled analogues limiting the maximum activity that can be administered without the induction of radiation nephrotoxicity. High kidney retention of MG analogues has been related to the N-terminal glutamic acids and could be substantially reduced by co-injection of polyglutamic acids[14] or of gelatin based plasma expander Gelofusine.[15] A different approach was followed by Good et al.[6] consisting of a systematic elimination of the glutamic acid residues present at the N-terminus of MG resulting in a reduction of negative charges. The authors demonstrated the positive correlation of the high kidney uptake and retention with increasing number of negative charges. The problem of very low metabolic stability in human serum[6] remains. These new findings prompted us to develop new DOTA-coupled MG analogues and to study

dx.doi.org/10.1021/jm101279a |J. Med. Chem. XXXX, XXX, 000–000

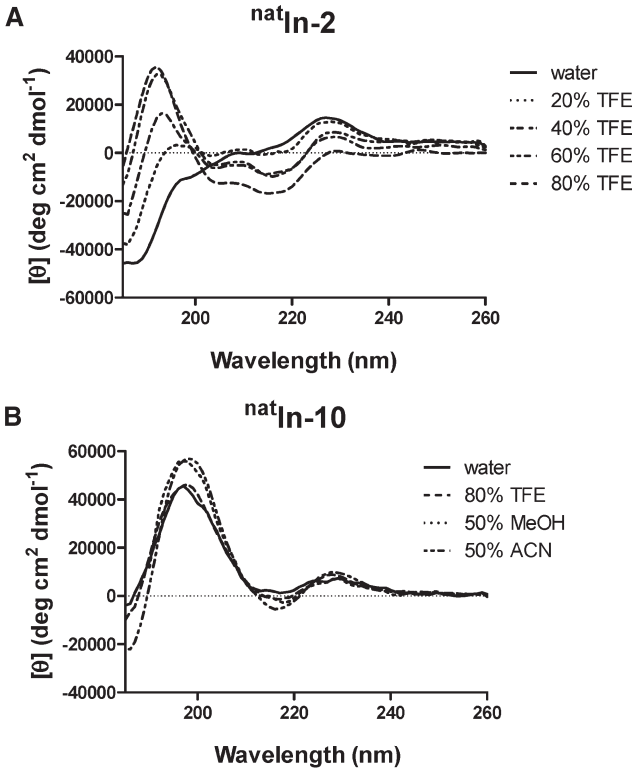

Figure 2. CD spectra of ^{nat}In-**2** (A) and ^{nat}In-**10** (B).

the effect of hydrophilic but nonionic spacers on tumor-to-kidney ratios and on enzymatic stability in human serum. We kept the seven C-terminal amino acids (in **8** we substituted Met with Nle), and as spacers we used PEG or D-amino acids like D-Ser and D-Gln. In this study the $T_{1/2}$ variation was almost 500-fold. Whereas increasing the number of dPEG and D-Ser has only very limited effect on serum stability, the number of D-Gln residues plays an important role in the stabilization of our analogues, showing a 65-fold half-life variation going from DOTA-(D-Gln)$_2$-gastrin-7 (**5**) to **10** (Table 2). These remarkable differences led us to investigate metabolic degradation in more detail. We chose one of the most labile MG analogues ^{111}In-**2** ($T_{1/2}$ = 1.7 ± 0.5 h) and its potential metabolites and incubated them in human blood serum and in EDTA-plasma and determined the composition of the metabolites. EDTA is known to deactivate metal-dependent enzymes.[16] The difference in half-lives when incubating ^{111}In-**2** in serum or in EDTA-plasma is indicative of different metabolic pathways. One pathway may be via ACE-like enzyme activity, where initial cleavage occurs between Met and Asp producing the metabolite E and the dipeptide Asp-Phe-NH$_2$.[17] E was not detected on HPLC because of its low stability, as previously described for the CCK-8 peptide. We detected the second cleavage point between Gly and Trp, which leaves ^{111}In-DOTA-PEG$_6$-Ala-Tyr-Gly-OH (D). Another cleavage point detected was between Tyr and Gly (C) resulting from the cleavage of E. Cleavage between Ala and Tyr seems to terminate this particular pathway. Another enzyme, probably an endopeptidase, releases gastrin-6.[18] When ^{111}In-**2** was incubated for 24 h in EDTA-plasma, C and D were not detected but only B. The incubation of C, D, and E in EDTA-plasma showed practically no degradation.

The degradation profile of ^{111}In-**6** with an intermediate stability shows the same pattern in serum and no metabolic degradation within 24 h in EDTA-plasma, which also supports the hypothesis of at least two different degradation pathways in the case of the metabolically labile analogues. ^{111}In-**10** reveals much higher stability and less metabolites compared with ^{111}In-**2**, which could imply that degradation via ACE-like enzyme activity is circumvented in the case of ^{111}In-**10**.

We hypothesized that circular dichroism measurements may give us a hint of the structural basis for the stability differences. This spectral technique helps to elucidate secondary structures of peptides and proteins in solution. We studied this for ^{nat}In-**2** and ^{nat}In-**10** to see if there are significant differences potentially explaining the stability differences. The spectrum of ^{nat}In-**2** in pure water argues for a random coil conformation; the aromatic groups on the amino acid side chains are responsible of the relatively high positive band between 225 and 230 nm. Addition of TFE led to spectral changes indicating stabilization of an α-helical conformation. The six D-Gln residues in the ^{nat}In-**10** sequence result in spectral bands characteristic of a type II reverse turn conformation, as reported by Reed et al.[13] The CD spectrum of this peptide does not show conformational changes even after addition of 80% of TFE or by dissolving it in different solvents. While for ^{nat}In-**2** there is no direct correlation between solvent properties and spectral characteristics, for ^{nat}In-**10** we notice the influence of the electronic charge distribution of the solvent molecules on the dissolved peptide with a fixed conformation. The higher intensities of the bands registered in methanol/water (1/1) and in acetonitrile/water (1/1) are due to the lower polarity of these mixtures compared to the 100% water or to the water/TFE mixtures. The relatively stable secondary structure of ^{nat}In-**10** is most likely responsible for a high metabolic stability and the difficulty of adopting a conformation easily fitting into the active site of the enzymes. The stable secondary structure adopted by ^{nat}In-**10** may explain its almost 2-fold higher internalization rate at 4 h compared to ^{nat}In-**2**.

Ca^{2+} mobilization results correlate with the internalization data showing that all the tested analogues trigger receptor internalization but the maximal response level is 2-fold smaller for **2** compared to the other analogues.

In addition to enhanced metabolic stability there is also significantly lower kidney uptake. A quantitative analysis of the biodistribution at 1, 4, 24, and 48 h showed similar biodistribution profiles for ^{111}In-**6** and ^{111}In-**10** with more favorable pharmacokinetics compared to highly charged ^{111}In-**11**. ^{111}In-**6** and ^{111}In-**10** show lower tumor uptake but by far lower kidney uptake and retention, which results in a 30-fold improvement of tumor-to-kidney ratio. A similar tumor-to-kidney ratio was observed for ^{111}In-DTPA-[D-Glu^1]-MG.[6] An almost 4-fold improvement in tumor uptake and a 3-fold improved tumor-to-kidney ratio was noted when the new analogues were compared to truncated ^{111}In-DOTA-DGlu-Glu-Ala-Tyr-Gly-Trp-Met-Asp-Phe-NH$_2$ (^{111}In-DOTA-MG10) and ^{111}In-DOTA-DGlu-Ala-Tyr-Gly-Trp-Met-Asp-Phe-NH$_2$ (^{111}In-DOTA-MG11) in the same animal model.[6] ^{111}In labeled peptides with nonionic D-Gln spacers exhibit highly improved pharmacokinetics. The first human study showed feasibility of ^{68}Ga-**10** to detect a gastrin receptor positive liver metastasis, but further studies are needed to establish if the high tumor-to-kidney ratio shown in our animal model will also be confirmed in humans.

There are two very important conclusions of these studies. The hydrophilic but nonionic D-Gln spacers increase the metabolic stability impressively. The length of spacers determines the metabolic stability. In addition the kidney uptake of some of

dx.doi.org/10.1021/jm101279a |J. Med. Chem. XXXX, XXX, 000–000

these radiopeptides is highly reduced resulting in an increased tumor-to-kidney ratio and a wider therapeutic window.

EXPERIMENTAL SECTION

General. All chemicals were obtained from commercial sources and used without additional purification. Rink amide 4-methylbenzhydrylalanine (MBHA) resin, Rink acid resin, Fmoc-protected amino acids, and Fmoc-PEG_{12}-OH are commercially available from NovaBiochem (Laeufelfingen, Switzerland). DOTA-tris(*t*-Bu ester) is commercially available (CheMatech Dijon, France). Fmoc-PEG_4-OH and Fmoc-PEG_6-OH were purchased from NeoMPS (Strasbourg, France) and $^{111}InCl_3$ from Covidien Medical (Petten, The Netherlands) or Perkin Elmer (Boston, MA, U.S.). DOTA-(D-Gln)$_3$-Ala-Tyr-Gly-Trp-Nle-Asp-Phe-NH_2 (**8**), DOTA-(D-Gln)$_4$-Ala-Tyr-Gly-Trp-Met-Asp-Phe-NH_2 (**9**), and DOTA-(D-Gln)$_6$-Ala-Tyr-Gly-Trp-Met-Asp-Phe-NH_2 (**10**) were purchased from Peptide Specialty Laboratories (Heidelberg, Germany).

The peptide−chelator conjugates were synthesized manually and purified by RP-HPLC on Metrohm HPLC system LC-CaDI 22-14 (Herisau, Switzerland) with a Macherey-Nagel VP 250/21 Nucleosil 100-5 C_{18} column (eluents A = 0.1% TFA in water and B = acetonitrile; gradient 0−20 min, 95−55% A; flow of 15 mL/min). All compounds were analyzed by RP-HPLC on a Hewlett-Packard system equipped with Macherey-Nagel Nucleosil 120 C_{18} column and UV detection at 215 nm (eluents A = 0.1% TFA in water and B = acetonitrile; gradient 0−20 min, 95−50% A; flow of 0.750 mL/min) to confirm purity of ≥95% and characterized by ESI-MS (Finnigan SSQ 7000 spectrometer, Bremen, Germany) and HRMS (Q-TOF Premier, Waters Micromass, Manchester, U.K.).

Quantitative γ counting was performed on a COBRA 5003 g-system well counter from Packard Instruments or 1470 Wizard from Wallac.

Cell Line. AR4-2J rat pancreatic tumor cells were obtained from ATCC (VA, U.S.) and cultured in Dulbecco's Modified Eagle medium (DMEM). DMEM was supplemented with vitamins, essential and nonessential amino acids, L-glutamine, antibiotics (penicillin/streptomycin), fungicide (amprotencine), and 10% fetal calf serum (FCS). All culture reagents were from Invitrogen (Basel, Switzerland) or from BioConcept (Allschwil, Switzerland).

Synthesis. The peptide−chelator conjugates were synthesized manually employing standard Fmoc strategy[23], using Rink amide MBHA.

Trt was used as protecting groups for D-Gln, Boc for Trp and D-Ser, and *t*-Bu for Asp and Tyr. The spacers and the prochelator DOTA(*t*-Bu)$_3$ were consecutively coupled to the peptide with *O*-(7-azabenzotriazol-1-yl)-*N*,*N*,*N*′,*N*′-tetramethyluronium (HATU) as activating agent. All the peptides were purified by semipreparative HPLC and characterized by ESI-MS and HRMS. The metabolites DOTA-PEG_6-Ala-OH, DOTA-PEG_6-Ala-Tyr-OH, DOTA-PEG_6-Ala-Tyr-Gly-OH, DOTA-PEG_6-Ala-Tyr-Gly-Trp-OH, DOTA-PEG_6-Ala-Tyr-Gly-Trp-Met-OH, DOTA-PEG_6-Ala-Tyr-Gly-Trp-Met-Asp-OH were assembled on Rink acid resin using the same protocol as described above.

The peptides **2** and **10** were complexed with $^{nat}InCl_3$ using the following procedure: a solution of DOTA-peptide conjugate (0.6 mmol) in 500 μL of sodium acetate buffer (0.4 M, pH 5.0) was incubated with 1.5 mmol of $InCl_3 \cdot 5H_2O$ for 30 min at 95°C and purified over a SepPak C18 cartridge preconditioned with 10 mL of MeOH and 10 mL of water. The cartridge was eluted with 10 mL of water followed by 7 mL of methanol, yielding ^{nat}In-DOTA-peptide conjugates after evaporation of the methanol. The pure product, obtained as a white powder (yields ranging from 70% to 80%) after lyophilization, was analyzed by analytical HPLC and characterized using ESI-MS.

Circular Dichroism. The CD measurements were performed at 25 °C using a Chirascan spectrometer. The instrument was purged with nitrogen gas at 20 L/min for 20 min before and during measurements. All spectra were recorded from 260 to 185 nm using a spectral bandwidth of 1 nm at 25 °C with a time constant of 3 s and a step resolution of 1 nm. CD data are given as mean residual molar ellipticities (θ in mdeg cm^2 dmol^{-1}). A quartz cell with a path length of 1 cm was used. The peptides were dissolved in H_2O to obtain a final concentration of 40 μmol/L. Samples spectra were recorded adding different percentages of TFE and different solvents.

Preparation of the Radiotracer. ^{111}In-DOTA-peptide conjugates were prepared by dissolving 5 or 10 μg of peptide in 250 μL of sodium acetate buffer (0.4 M, pH 5.0) and incubating the peptide solution with $^{111}InCl_3$ (37−185 MBq) for 30 min at 95 °C. Quality control was performed using radio-HPLC. To obtain structurally characterized homogenous ligands, 1 equiv of $^{nat}InCl_3 \cdot 5H_2O$ was added and the final solution incubated again at 95 °C for 30 min. For biodistribution and serum stability studies, the labeling was performed accordingly without the addition of cold metal. For injection, the radioligand solution was prepared by dilution with 0.9% NaCl.

^{68}Ga-**10** was prepared using 500−750 MBq of $^{68}GaCl_3$ obtained from a ^{68}Ge/^{68}Ga generator (Cyclotron Co., Obninsk, Russia). The eluate was preconcentrated and purified from potential metallic impurities on cation exchange column (50W-X8, <400 mesh, Bio-Rad AG, Munich, Germany). For elution 98% acetone/0.05 mol/L HCl (400 μL) was used. This was added to 4 mL of water containing 25 μg (12 nmol) of **10** and heated at 100°C for 10 min. The reaction mixture was purified using a Sep-Pak C18 cartridge, which was washed with 5 mL of water, followed by 0.5 mL of ethanol, and diluted in 5 mL of saline. After sterile filtration quality control was performed using HPLC and thin-layer chromatography. For patient study radiopharmaceutical with radiochemical yield of >95% was used.

Binding Affinity Studies on CCK-1 and Gastrin-Receptor Expressing Tissues. Binding affinities were evaluated as described[19] in surgically resected human tumor tissues selected from previous experiments to express CCK-1 or gastrin receptors.[2] Increasing amounts of MG derivatives were added to the ^{125}I-CCK containing incubation medium to generate competitive inhibition curves. Tissue slides were exposed to Biomax MR films (Kodak) for 7 days. Autoradiograms were quantified using tissue standards for iodinated compounds (Amersham, U.K.).[20]

Enzymatic Stability in Human Serum and Identification of Metabolites. To 1 mL of fresh human serum, previously equilibrated in a 5% CO_2 environment at 37 °C, 0.6 nmol of ^{111}In-labeled peptide was added. The mixture was incubated in a 5% CO_2, 37 °C environment. At different time points, 100 μL aliquots were removed and treated with 200 μL of EtOH to precipitate serum proteins. Samples were centrifuged for 10 min at 1850*g*. An amount of 100 μL of supernatant was removed for activity counting in a γ-well counter. The sediment was washed twice with 1 mL of EtOH. The activity in the supernatant was compared with the activity in the pellet to give the percentage of peptides bound to proteins or radiometal transferred to serum proteins. The supernatant was analyzed with radio-HPLC to determine the relative amount of intact peptide and its metabolites in serum. Half-life was calculated fitting a first order reaction to the experimental data (eq 1) using OriginPro 7.5G (Microcal Software, Inc., Northampton, MA).

$$[A] = e^{-k_1 t} \quad (1)$$

To identify the metabolites, we choose the metabolically labile ^{111}In-**2** as a leading peptide. The extracted supernatant, obtained as described above, was co-injected with the potential metabolites, synthesized as described above. Using OriginPro 7.5G (Microcal Software, Inc., Northampton, MA), we established formation and disappearance rates of metabolites, fitting experimental data to eq 2 (see Table 1S).

$$[M] = \frac{k_{form}}{k_{form} - k_{disapp}}(e^{-k_{disapp} t} - e^{-k_{form} t}) \quad (2)$$

To follow metabolic pathways of each individual metabolite they were added to the serum and handled in the same way as the lead peptide. To try

dx.doi.org/10.1021/jm101279a |J. Med. Chem. XXXX, XXX, 000–000

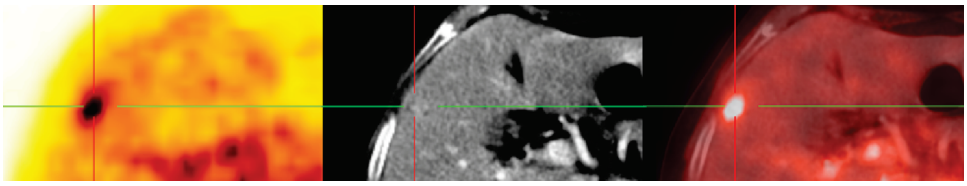

Figure 3. PET/CT scan performed 70 min after iv infusion (15 min) of ^{68}Ga-**10** (347 MBq) (from left to right): PET scan, CT scan, fused image.

to establish if there are metallopeptidases involved in metabolic degradation, ^{111}In-**2** and its metabolites were also studied in EDTA-plasma.

In Vitro Internalization and Cellular Retention Studies Using AR4-2J Cell Line. The AR4-2J cells were seeded at a density of 0.5−1.0 million cells/well in six-well plates and incubated overnight to obtain good cell adherence. On the day of the experiment, cells were treated exactly as described recently.[21]

Calcium Mobilization Assay. Intracellular calcium mobilization was measured in AR4-2J cells using the calcium 3 assay kit (Molecular Probes, Inc.) following the protocol described earlier.[22]

In brief, AR4-2J cells (50 000 cells per well) were seeded in 96-well plates and cultured for 1 day at 37 °C and 5% CO_2. On the day of the experiment, the medium was removed and the cells were then loaded with 100 μL per well of Ca dye in assay buffer (Hank's balanced salt solution and 20 mM 2-[4-(2-hydroxyethyl)-1- piperazinyl]ethanesulfonic acid (HEPES)) containing 2.5 mM probenecid for 1 h at 37 °C. One to three serial dilutions of the peptides, in a dilution buffer (HBSS with 20 mM HEPES, 0.1% BSA, 0.05% pluronic acid), starting from 6 mM were loaded in the 96-well plate. The plates were loaded into a FLEX station 3 microplate reader (Molecular Devices). Intracellular calcium mobilization was recorded at room temperature for 4 min in a kinetic monitoring fluorescence emission at 525 nm (with λ_{ex} = 485 nm), and the data were analyzed by SoftMax Pro software (Molecular Devices). The instrument was programed such that the agonist (20 mL at varying concentrations), added to cell plates, is diluted 1:6 times. Maximum fluorescence (F_{max}) was measured after the addition of ionomycin. Baseline (control) measurements were taken for untreated cells. EC_{50} and maximal response for each compound were calculated.

Biodistribution Experiments in AR4-2J Tumor Bearing Lewis Rats. All animal experiments were performed in compliance with the Swiss regulation for animal treatment (Permit No. 789). Lewis male rats were implanted subcutaneously with 10 million AR4-2J tumor cells, which were freshly expanded in a sterilized phosphate-buffered saline (PBS, pH 7.4) solution. At 11−16 days after inoculation the rats were injected into tail vein with 0.1 nmol of ^{111}In-radiolabeled peptide (about 1.1 MBq dissolved in 200 μL of 0.9% NaCl solution). For the determination of nonspecific uptake in tumor or receptor positive organs, a group of animals was co-injected with 100 nmol of unlabeled **10** in 0.9% NaCl solution. At selected time points the rats (in groups of 2−10) were sacrificed and organs of interest were collected, rinsed of excess blood, plotted dry, weighed, and counted in a γ-counter. The total counts injected per animal were determined by extrapolation from counts of an aliquot taken from the injected solution as a standard. Uptake of different organs was calculated as percentage of injected activity per gram tissue (% IA/g).

Patient Study. Whole body PET/CT scan of a 59-year-old female patient with medullary thyroid carcinoma (MTC) was performed on Siemens Biograph Duo (Siemens, Germany) 70 min after slow injection of 347 MBq ^{68}Ga-**10** over 15 min (Figure 3). The administration of the peptide (~20 μg), performed under continuous monitoring of the patient, was tolerated without any adverse effects.

Statistical Methods. Data are expressed as the mean ± standard deviation, which were calculated with Microsoft Excel. To compare differences between groups, the Student's t test was used. $p < 0.01$ was considered to be statistically significant.

■ ASSOCIATED CONTENT

Supporting Information. Metabolite formation and disappearance rates for ^{111}In-**2**; biodistribution data of ^{111}In-**6**, ^{111}In-**10**, and ^{111}In-**11**; intracellular calcium mobilization induced in AR4-2J cells by minigastrin analogues; PET/CT scan of gastrin receptor positive liver metastases. This material is available free of charge via the Internet at http://pubs.acs.org.

■ AUTHOR INFORMATION

Corresponding Author

*Phone: ++49 761 270 7422. Fax: ++49 761 270 3930. E-mail: helmut.maecke@uniklinik-freiburg.de.

■ ACKNOWLEDGMENT

We thank Prof. H. Wennemers and Dr. M. Kümin for support with the CD measurements, Novartis Pharma for analytic assistance, S. Tschumi for her expert technical help, and the COST BM0607 action. Financial support from the European Community for the TARCC Project within the 7th Framework Program and from the Swiss National Science Foundation (Grant 320000-11833) is gratefully acknowledged.

■ REFERENCES

(1) Dufresne, M.; Seva, C.; Fourmy, D. Cholecystokinin and gastrin receptors. *Physiol. Rev.* **2006**, *86*, 805–847.

(2) Reubi, J. C.; Schaer, J. C.; Waser, B. Cholecystokinin(CCK)-A and CCK-B/gastrin receptors in human tumors. *Cancer Res.* **1997**, *57*, 1377–1386.

(3) Gotthardt, M.; Behe, M. P.; Beuter, D.; Battmann, A.; Bauhofer, A.; Schurrat, T.; Schipper, M.; Pollum, H.; Oyen, W. J.; Behr, T. M. Improved tumour detection by gastrin receptor scintigraphy in patients with metastasised medullary thyroid carcinoma. *Eur. J. Nucl. Med. Mol. Imaging* **2006**, *33*, 1273–1279.

(4) Froberg, A. C.; de Jong, M.; Nock, B. A.; Breeman, W. A.; Erion, J. L.; Maina, T.; Verdijsseldonck, M.; de Herder, W. W.; van der Lugt, A.; Kooij, P. P.; Krenning, E. P. Comparison of three radiolabelled peptide analogues for CCK-2 receptor scintigraphy in medullary thyroid carcinoma. *Eur. J. Nucl. Med. Mol. Imaging* **2009**, *36*, 1265–1272.

(5) Behe, M.; Behr, T. M. Cholecystokinin-B (CCK-B)/gastrin receptor targeting peptides for staging and therapy of medullary thyroid cancer and other CCK-B receptor expressing malignancies. *Biopolymers* **2002**, *66*, 399–418.

(6) Good, S.; Walter, M. A.; Waser, B.; Wang, X.; Muller-Brand, J.; Behe, M. P.; Reubi, J. C.; Maecke, H. R. Macrocyclic chelator-coupled gastrin-based radiopharmaceuticals for targeting of gastrin receptor-expressing tumours. *Eur. J. Nucl. Med. Mol. Imaging* **2008**, *35*, 1868–1877.

(7) Breeman, W. A.; Froberg, A. C.; de Blois, E.; van Gameren, A.; Melis, M.; de Jong, M.; Maina, T.; Nock, B. A.; Erion, J. L.; Macke, H. R.; Krenning, E. P. Optimised labeling, preclinical and initial clinical aspects of CCK-2 receptor-targeting with 3 radiolabeled peptides. *Nucl. Med. Biol.* **2008**, *35*, 839–849.

(8) Mather, S. J.; McKenzie, A. J.; Sosabowski, J. K.; Morris, T. M.; Ellison, D.; Watson, S. A. Selection of radiolabeled gastrin analogs for peptide receptor-targeted radionuclide therapy. *J. Nucl. Med.* **2007**, *48*, 615–622.

(9) von Guggenberg, E.; Sallegger, W.; Helbok, A.; Ocak, M.; King, R.; Mather, S. J.; Decristoforo, C. Cyclic minigastrin analogues for gastrin receptor scintigraphy with technetium-99m: preclinical evaluation. *J. Med. Chem.* **2009**, *52*, 4786–4793.

(10) Sosabowski, J. K.; Matzow, T.; Foster, J. M.; Finucane, C.; Ellison, D.; Watson, S. A.; Mather, S. J. Targeting of CCK-2 receptor-expressing tumors using a radiolabeled divalent gastrin peptide. *J. Nucl. Med.* **2009**, *50*, 2082–2089.

(11) Garcia Garayoa, E.; Schweinsberg, C.; Maes, V.; Brans, L.; Blauenstein, P.; Tourwe, D. A.; Schibli, R.; Schubiger, P. A. Influence of the molecular charge on the biodistribution of bombesin analogues labeled with the $[^{99m}Tc(CO)_3]$-core. *Bioconjugate Chem.* **2008**, *19*, 2409–2416.

(12) Woody, R. W. Contributions of tryptophan side chains to the far-ultraviolet circular dichroism of proteins. *Eur. Biophys. J.* **1994**, *23*, 253–262.

(13) Reed, J.; Reed, T. A. A set of constructed type spectra for the practical estimation of peptide secondary structure from circular dichroism. *Anal. Biochem.* **1997**, *254*, 36–40.

(14) Behe, M.; Kluge, G.; Becker, W.; Gotthardt, M.; Behr, T. M. Use of polyglutamic acids to reduce uptake of radiometal-labeled minigastrin in the kidneys. *J. Nucl. Med.* **2005**, *46*, 1012–1015.

(15) Gotthardt, M.; van Eerd-Vismale, J.; Oyen, W. J.; de Jong, M.; Zhang, H.; Rolleman, E.; Maecke, H. R.; Behe, M.; Boerman, O. Indication for different mechanisms of kidney uptake of radiolabeled peptides. *J. Nucl. Med.* **2007**, *48*, 596–601.

(16) Auld, D. S. Removal and replacement of metal ions in metallopeptidases. *Methods Enzymol.* **1995**, *248*, 228–242.

(17) Dubreuil, P.; Fulcrand, P.; Rodriguez, M.; Laur, J.; Bali, J. P.; Martinez, J. ACE-like hydrolysis of gastrin analogs and CCK-8 by fundic mucosal cells of different species with release of the amidated C-terminal dipeptide. *Biochim. Biophys. Acta* **1990**, *1039*, 171–176.

(18) Palnaes Hansen, C.; Stadil, F.; Rehfeld, J. F. Metabolism and acid secretory effect of sulfated and nonsulfated gastrin-6 in humans. *Am. J. Physiol.: Gastrointest. Liver Physiol.* **2000**, *279*, G903–G909.

(19) Reubi, J. C.; Waser, B.; Schaer, J. C.; Laederach, U.; Erion, J.; Srinivasan, A.; Schmidt, M. A.; Bugaj, J. E. Unsulfated DTPA- and DOTA-CCK analogs as specific high-affinity ligands for CCK-B receptor-expressing human and rat tissues in vitro and in vivo. *Eur. J. Nucl. Med.* **1998**, *25*, 481–490.

(20) Erchegyi, J.; Cescato, R.; Grace, C. R.; Waser, B.; Piccand, V.; Hoyer, D.; Riek, R.; Rivier, J. E.; Reubi, J. C. Novel, potent, and radioiodinatable somatostatin receptor 1 (sst1) selective analogues. *J. Med. Chem.* **2009**, *52*, 2733–2746.

(21) Zhang, H.; Chen, J.; Waldherr, C.; Hinni, K.; Waser, B.; Reubi, J. C.; Maecke, H. R. Synthesis and evaluation of bombesin derivatives on the basis of pan-bombesin peptides labeled with indium-111, lutetium-177, and yttrium-90 for targeting bombesin receptor-expressing tumors. *Cancer Res.* **2004**, *64*, 6707–6715.

(22) Cescato, R.; Maina, T.; Nock, B.; Nikolopoulou, A.; Charalambidis, D.; Piccand, V.; Reubi, J. C. Bombesin receptor antagonists may be preferable to agonists for tumor targeting. *J. Nucl. Med.* **2008**, *49*, 318–326.

(23) Atherton, E.; Sheppard, R. Fluorenylmethoxycarbonyl-polyamide Solid Phase Peptide Synthesis. General Principles and Development. In *Solid Phase Peptide Synthesis. A Practical Approach*; Oxford Information Press: Oxford, U.K., 1989; pp 25−38.